Syntaxin 3, but not syntaxin 4, is required for mast cell–regulated exocytosis, where it plays a primary role mediating compound exocytosis

Received for publication, August 23, 2018, and in revised form, November 30, 2018 Published, Papers in Press, December 18, 2018, DOI 10.1074/jbc.RA118.005532

Elizabeth Sanchez[‡§], Erika A. Gonzalez[‡§], David S. Moreno[‡§], Rodolfo A. Cardenas[‡§], Marco A. Ramos[‡§], Alfredo J. Davalos[‡§], John Manllo[‡§], Alejandro I. Rodarte[‡§], Youlia Petrova[‡], Daniel C. Moreira[‡§], Miguel A. Chavez[‡§], Alejandro Tortoriello[‡§], Adolfo Lara[¶], Berenice A. Gutierrez[‡§], Alan R. Burns[‖], Ruth Heidelberger[¶], and Roberto Adachi[‡1]

From the [‡]Department of Pulmonary Medicine, University of Texas M.D. Anderson Cancer Center, Houston, Texas 77030, [§]Tecnologico de Monterrey, Escuela de Medicina y Ciencias de la Salud, Monterrey, Nuevo León 64710, México, the [¶]Department of Neurobiology and Anatomy, McGovern Medical School at the University of Texas Health Science Center, Houston, Texas 77030, and the [‖]College of Optometry, University of Houston, Houston, Texas 77204

Edited by Peter Cresswell

Mast cells (MCs) participate in allergy, inflammation, and defense against pathogens. They release multiple immune mediators via exocytosis, a process that requires SNARE proteins, including syntaxins (Stxs). The identity of the Stxs involved in MC exocytosis remains controversial. Here, we studied the roles of Stx3 and -4 in fully developed MCs from conditional knockout mice by electrophysiology and EM, and found that Stx3, and not Stx4, is crucial for MC exocytosis. The main defect seen in Stx3-deficient MCs was their inability to engage multigranular compound exocytosis, while leaving most single-vesicle fusion events intact. We used this defect to show that this form of exocytosis is not only required to accelerate MC degranulation but also essential to achieve full degranulation. The exocytic defect was severe but not absolute, indicating that an Stx other than Stx3 and -4 is also required for exocytosis in MCs. The removal of Stx3 affected only regulated exocytosis, leaving other MC effector responses intact, including the secretion of cytokines via constitutive exocytosis. Our *in vivo* model of passive systemic anaphylaxis showed that the residual exocytic function of Stx3-deficient MCs was sufficient to drive a full anaphylactic response in mice.

Mast cells (MCs)[2] are key effectors of adaptive and innate immunity, and modulators of local inflammation (1). Armed with prominent electron-dense granules loaded with inflammatory mediators (2, 3), and strategically located in the host peripheral tissues, they degranulate upon exposure to a variety of stimuli (4–6). MC degranulation is one of the best examples of regulated exocytosis, where the preformed contents are stored in secretory granules and released only after a specific stimulus (7, 8). The MC constitutes a premier system to study regulated exocytosis at high resolution due to their large granules and the predictable and almost complete degranulation after stimulation (9). Regulated exocytosis in MCs can use single-vesicle and compound exocytosis (10). In single-vesicle exocytosis, each secretory vesicle fuses independently with the plasma membrane. In sequential compound exocytosis, vesicles lying deeper within the cell fuse with vesicles already fused with the plasma membrane. In multigranular compound exocytosis, vesicles fuse homotypically with each other before fusing with the plasma membrane (11). MCs secrete products via constitutive exocytosis too. This involves the continuous traffic of vesicles from the Golgi apparatus to the plasma membrane, and the amount of secreted product depends on the rate of synthesis of the vesicle cargo (12). MCs also have secretory responses that are independent of exocytosis, such as secretion of eicosanoids, which are exported via plasma membrane transporters (13).

As any other form of exocytosis, the molecular machinery that mediates MC degranulation should involve SNARE (soluble *N*-ethylmaleimide-sensitive factor attachment receptor) proteins, including syntaxins (Stxs) (14). Stxs are a subset of SNARE proteins located on the target membrane, in this case the plasma membrane. Among all of the members of the Stx family, Stx1a, -1b, -2, -3, -4, and -11 mediate exocytosis in different mammalian cells (15, 16). The helical SNARE domain

This work was supported by National Institutes of Health Grants AI093533, CA016672, EY007551, and EY012128. The authors declare that they have no conflicts of interest with the contents of this article. The content is solely the responsibility of the authors and does not necessarily represent the official views of the National Institutes of Health.

This article contains Figs. S1 and S2.

[1] To whom correspondence should be addressed: Dept. of Pulmonary Medicine, University of Texas M.D. Anderson Cancer Center, 2121 W. Holcombe Blvd., Houston, TX 77030. Tel.: 713-563-0410; Fax: 713-563-0411; E-mail: radachi@mdanderson.org.

[2] The abbreviations used are: MC, mast cell; B6, C57BL6/J mouse line; BMMC, bone marrow-derived MC; cKO, conditional KO; C_m, capacitance; ΔC_m, capacitance gain; DNP, 2,4-dinitrophenol; F, farad; FLP, Flp recombinase; FRT, Flp recognition target site; G_m, membrane conductance; G_s, series conductance; GTPγS, guanosine 5′-3-*O*-(thio)triphosphate; HSA, human serum albumin; IL, interleukin; i.p., intraperitoneally; LTC_4, leukotriene C_4; Munc, mammalian homolog of *C. elegans* uncoordinated gene; Neo, neomycin phosphotransferase; PCMC, peritoneal cell-derived MC; PGD_2, prostaglandin D_2; PGK, phosphoglucokinase promoter; PI, PMA plus ionomycin; PMA, phorbol 12-myristate 13-acetate; RBL-2H3, rat basophilic leukemia cell line; S, siemens; SNAP23/25, synaptosomal-associated protein 23 or 25; SNARE, soluble *N*-ethylmaleimide–sensitive factor attachment protein receptor; Stx, syntaxin; *Sv*, surface density; TNF, tumor necrosis factor; VAMP, vesicle-associated membrane protein; *Vv*, volume density; Wsh, MC-deficient kit$^{W\text{-}sh/W\text{-}sh}$ mouse.

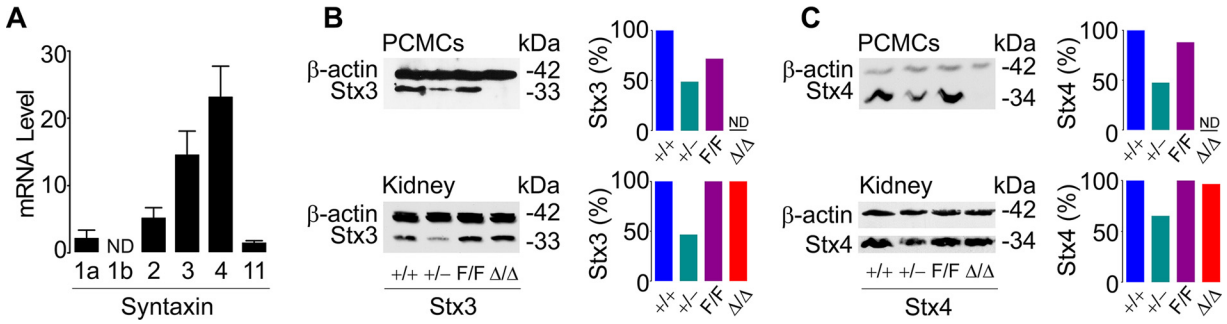

Figure 1. Expression of exocytic Stxs in MCs. *A*, quantitative RT-PCR of B6 peritoneal MCs for Stx1a, -1b, -2, -3, -4, and -11 relative to β-actin. *ND*, not detected; $n = 3$; *bar*, mean; *error bar*, S.E. Representative immunoblots of PCMC and kidney lysates are shown for Stx3 (*B*) and Stx4 (*C*). β-Actin was used as loading control. *Bar graph insets*, densitometry relative to β-actin and +/+.

of an exocytic Stx associates with the SNARE domains of SNAP23/25 (synaptosomal-associated protein 23 or 25) and VAMP (vesicle-associated membrane protein) to form the SNARE complex, which is essential for fusion of the vesicle membrane and plasma membrane (17). The formation and function of this complex requires the coordinated participation of members of the Munc (mammalian isoform of the uncoordinated gene of *Caenorhabditis elegans*) 13, Munc18, complexin, and synaptotagmin families (18).

We have described that in mature MCs, regulated exocytosis depends on synaptotagmin-2 (19), Munc13-2 and -4 (20), and Munc18-2 (21, 22). About the Stxs involved in this process, it has been accepted for more than a decade (23, 24) that Stx4 is an essential participant in MC exocytosis, based on multiple studies on RBL-2H3 cells (25–29), rat peritoneal MCs (30), and human intestine-derived MCs (31). However, these findings have been questioned by others (32–34). Stx3, a SNARE protein that is localized both in the plasma and granule membranes (35), has also been shown to play an important role in exocytosis in RBL-2H3 cells (36–39) and human intestine-derived MCs (40). The main caveats with these studies, some with opposite findings, are that the interference with expression or function of Stx was only partial, few tested Stx3 and -4 in the same experimental paradigms, none dissected the effects on compound exocytosis, and most relied on cell lines. We found that interfering with expression of synaptotagmin-2 (41) and Munc18-1 (42, 43) in RBL-2H3 cells had different effects on exocytosis than their elimination in mature MCs (19, 22). Thus, we chose to interrogate the impact of complete removal of Stx3 and Stx4 on single-vesicle and compound exocytosis in fully developed MCs.

To study the roles of Stx3 and Stx4 *in vivo*, we created conditional KO (cKO) mice for both genes. We could not find any role for Stx4 in MC exocytosis in any of our assays. Removal of Stx3 decreased the amount and rate of exocytosis mainly because multigranular compound exocytosis was almost completely eliminated, leaving single-granule secretion mostly intact. This defect affected exclusively the secretion of granule contents and not the secretion of cytokines or eicosanoids. Unlike what we have seen in the absence of Munc13-4 (20) and Munc18-2 (22), elimination of Stx3 in MCs did not affect the anaphylactic response.

Results

Expression of Stxs in MCs and generation of conditional KO mice

Given the importance of MC degranulation in inflammatory responses, we decided to study the Stxs that mediate this process. We used the expression pattern of the exocytic Stxs in C57BL/6J (B6) MCs to choose the Stxs for our first study. We noted that the main isoforms present in peritoneal MCs were Stx3 and -4 (Fig. 1*A*) and targeted both for deletion.

For Stx3, we used an ES clone with a gene trap in intron 1 of *Stx3* (Fig. S1*A*). This cassette, which contains a splice acceptor site, interrupts the transcription of Stx3. Heterozygous mice generated from ES cells with this mutant allele were crossed with FLP-expressing mice to invert the cassette, allowing Stx3 expression but retaining two flanking loxP sites ("floxed" or F allele) that render it susceptible to another inversion by Cre recombinase. This final inversion blocks the expression of Stx3 and "locks" the allele (*i.e.* it cannot be inverted again). To target Stx4 (Fig. S1*B*), we introduced by homologous recombination two loxP sites flanking exons 1–4 of *Stx4* (F allele). Cre recombination removes the translation initiation codon. In both cases, Cre recombination was predicted to eliminate expression of the targeted gene. We crossed $Stx3^{F/F}$ and $Stx4^{F/F}$ mice with B6.C-Tg(CMV-cre)1Cgn/J mice to generate germ line (global or constitutive) deletants (−allele) or with Tg(Cma1-cre) ARoer mice to remove expression only in MCs (Δ allele). We have shown the efficacy of this strategy before (20).

All of our genetic manipulations were confirmed by PCR (Fig. S1, *C* and *D*). Both global deletants were embryonically lethal. Crosses among $Stx3^{+/-}$ mice produced 39 $Stx3^{+/+}$ and 61 $Stx3^{+/-}$ mice, but no $Stx3^{-/-}$ mice. Similar crosses among $Stx4^{+/-}$ mice produced 44 $Stx4^{+/+}$, 72 $Stx4^{+/-}$, and 0 $Stx4^{-/-}$ mice. $Stx3^{+/-}$, $Stx3^{F/F}$, $Stx3^{\Delta/\Delta}$, $Stx4^{+/-}$, $Stx4^{F/F}$, and $Stx4^{\Delta/\Delta}$ mice were viable, fertile, transmitted the mutant allele following a Mendelian pattern, and had no gross abnormalities and a normal life span when raised in a specific pathogen-free facility.

Immunoblots from peritoneal cell-derived MCs (PCMCs) and other tissues confirmed the reduced expression of the targeted Stx in +/− animals and their normal expression in F/F mice. They also confirmed that recombination by Cre activity removed expression of the targeted gene and demonstrated the specificity of the deletion in Δ/Δ mice only in MCs (Fig. 1, *B* and *C*). Because it

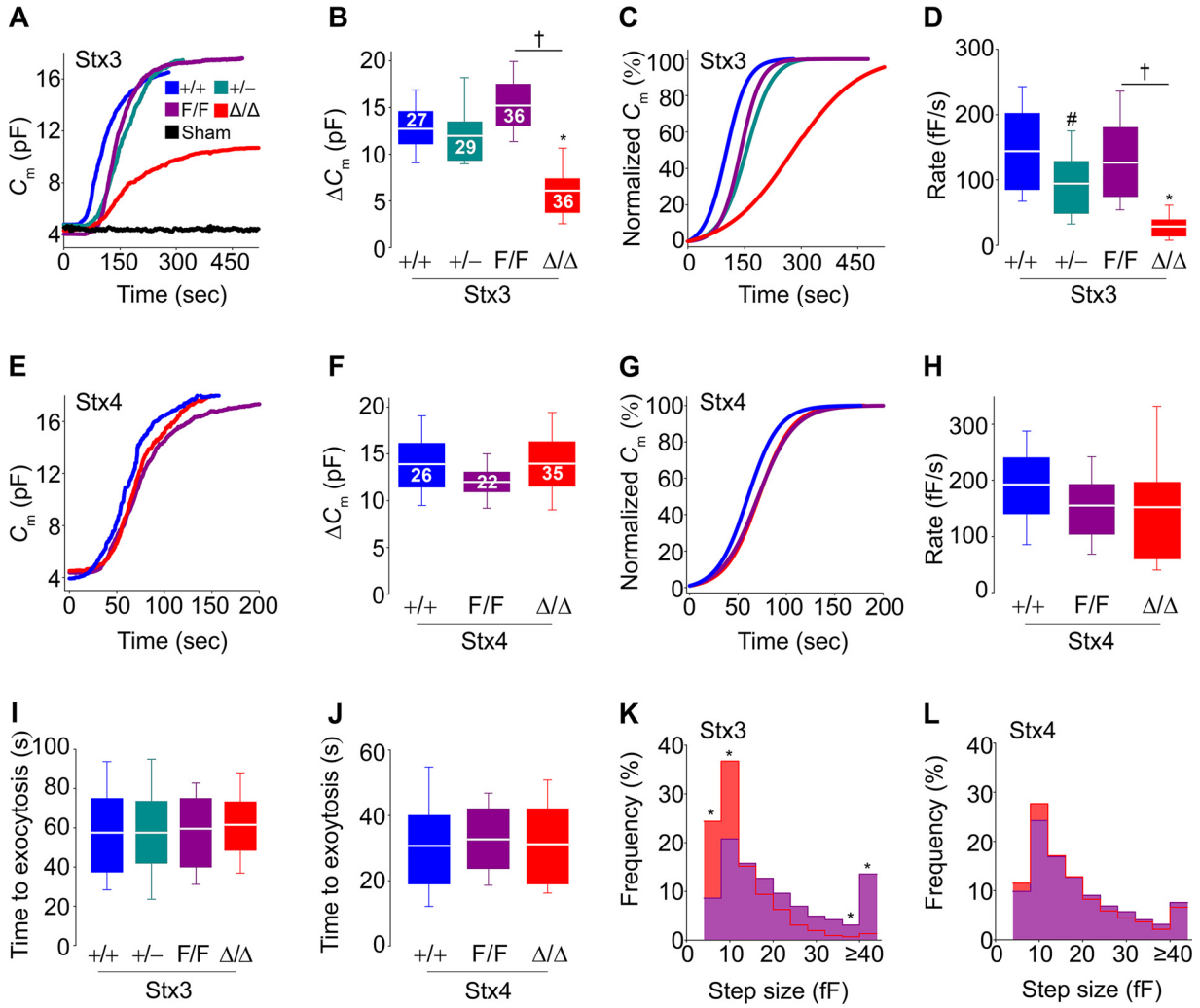

Figure 2. Absence of Stx3, but not Stx4, influences the amount, rate, and size of vesicles exocytosed in MCs. Shown are C_m recordings of individual peritoneal MCs after stimulation by intracellular dialysis of GTPγS and Ca^{2+}. Access to the cell interior was obtained via establishment of the whole-cell recording configuration at time 0. *Sham*, +/+ MCs dialyzed with a solution lacking GTPγS. The *color key* in *A* applies to *all panels*. *A* and *E*, representative traces of C_m recordings. *B* and *F*, ΔC_m after stimulation. *Numbers inside boxes* in *B* and *F*, number of cells studied, obtained from 6–8 animals of each genotype; applies to *D*, *H*, and *I–L*. *C* and *G*, representative normalized C_m traces. *D* and *H*, rate of exocytosis between 40 and 60% of total ΔC_m. *I* and *J*, time between cell access and beginning of the exocytic burst. *K* and *L*, frequency distribution of C_m step sizes between 1 and 15% of total ΔC_m. Signals < 4 fF have been removed for clarity. *White line*, mean; *box*, 25th–75th percentile; *whiskers*, 5th–95th percentile. #, $p \leq 0.05$; †, $p \leq 0.01$; *, $p \leq 0.001$; all compared with +/+ MCs unless otherwise specified.

has been shown that sometimes the expression of an Stx can affect the expression of its cognate Munc18 protein (44), we tested how expression of Stx3 affected the expression of Munc18−2 and found no differences among MCs from all Stx3 mutant mice (Fig. S2).

Absence of Stx3, but not Stx4, hinders the extent and kinetics of exocytosis in MCs

To determine the effects of lacking Stx3 or Stx4 on MC exocytosis at high resolution, we measured plasma membrane capacitance (C_m) in single peritoneal MCs using the whole-cell patch clamp configuration (9, 10, 45, 46). In this assay, the intracellular dialysis of GTPγS and Ca^{2+} through the patch pipette induces almost complete MC degranulation, and the resolution is such that single fusion events can be identified (9, 45). C_m is proportional to the area of the plasma membrane. During exocytosis, a secretory vesicle incorporates its membrane into the plasma membrane, and this increase in area of the plasma membrane is recorded as an increase in C_m (ΔC_m) (45). In all of the studied MCs, the mean baseline C_m was 5.7 ± 0.5 pF (mean ± S.E.), and the average final intracellular [Ca^{2+}] measured using Fura-2 fluorescence was 434 ± 36 nM, and we found no differences in these two values among all Stx3 and Stx4 genotypes. C_m recordings in $Stx3^{+/+}$ MCs with a pipette loaded with an intracellular solution with no GTPγS showed that intracellular access by itself did not induce exocytosis (Fig. 2*A*, *black trace*). The ΔC_m among $Stx3^{+/+}$, $Stx3^{+/-}$, and $Stx3^{F/F}$ MCs was almost identical, but it was significantly decreased in $Stx3^{\Delta/\Delta}$ MCs (Fig. 2, *A* and *B*). Curves were normalized (Fig. 2*C*) to calculate the maximum rate of exocytosis (rate between 40 and 60% of total ΔC_m). Although they achieved the same total ΔC_m, $Stx3^{+/-}$ MCs did so at a significantly lower rate compared with $Stx3^{+/+}$ MCs, a gap that was even larger between $Stx3^{F/F}$ and $Stx3^{\Delta/\Delta}$ MCs (Fig. 2*D*).

In contrast to the clear phenotype we found in Stx3-deficient MCs, deletion of Stx4 had no effects on the magnitude and speed of exocytosis (Fig. 2, *E–H*).

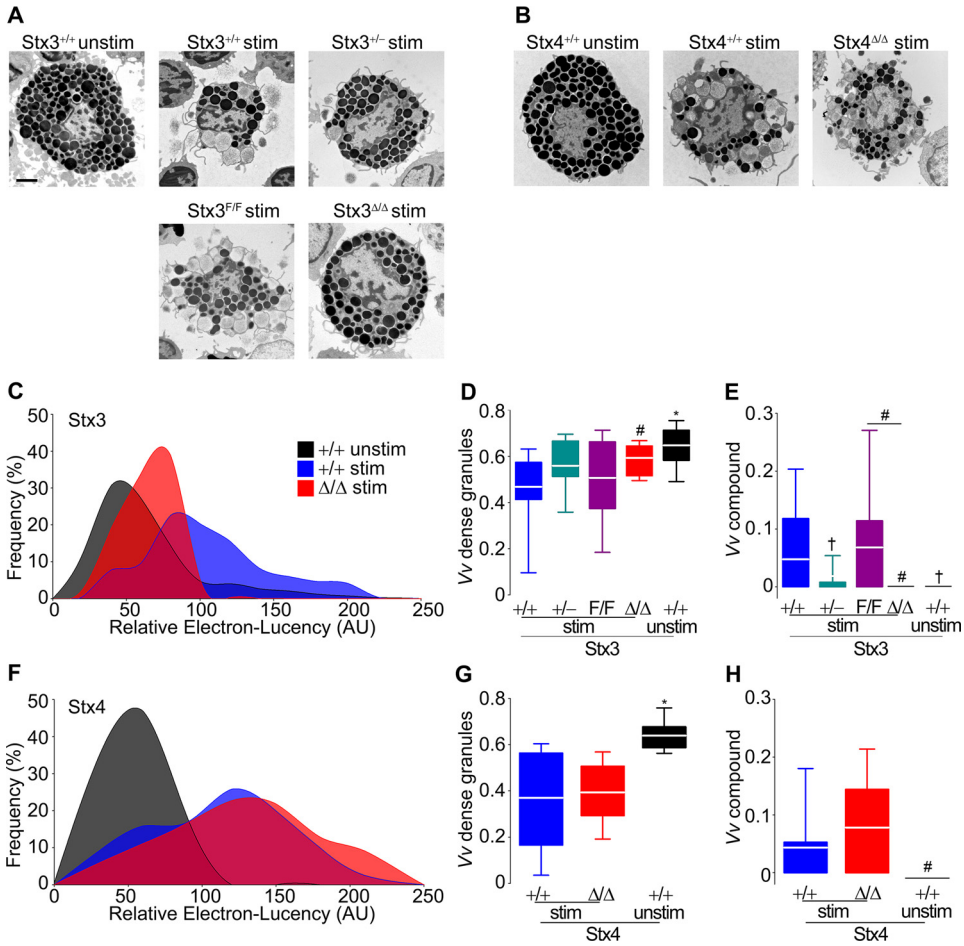

Figure 3. Absence of Stx3, but not Stx4, alters the ultrastructural changes associated with exocytosis in MCs. Peritoneal MCs that were stimulated with PMA/ionomycin for 5 min (*stim*) or left unstimulated (*unstim*) were studied under EM. *AU*, arbitrary units. *A* and *B*, representative cell profiles. *Scale bar*, 2 μm. *C* and *F*, relative electron lucency of MC granules based on a 0 (*black*) to 255 (white) *grayscale*. The *color key* in *C* applies to *F*. *D* and *G*, *Vv* of electron-dense granules (electron lucency < 120). *E* and *H*, *Vv* of compound compartments. $n = \sim 30$ granules/cell, 25 cells/animal, 6 animals/genotype. *White line*, mean; *box*, 25th–75th percentile; *whiskers*, 5th–95th percentile. #, $p \leq 0.05$; †, $p \leq 0.01$; *, $p \leq 0.001$; all compared with +/+ stimulated MCs unless otherwise specified.

We also measured the time between cell access and initial rise in C_m to test whether absence of expression of Stx3 or Stx4 affected the interval between stimulus and response. Unlike the significant delay we observed in Munc13-4–deficient MCs (20), we found no alterations in the absence of these Stxs (Fig. 2, *I* and *J*).

The slower rate of exocytosis in Stx3-deficient MCs could be due to a reduction of the number of granules being exocytosed per unit of time, to a decrease in the size of the vesicles fusing with the plasma membrane, or both. Each "step" in the C_m curve represents the fusion of a single vesicle, and the size of each "step" is proportional to the surface area (and thus the volume) of the fusing vesicle (45). By comparing MCs from $Stx3^{F/F}$ and $Stx3^{\Delta/\Delta}$ mice, we noted a significant shift to exocytosis of smaller-sized vesicles in the absence of Stx3 (Fig. 2*K*). We noted that ~70% of steps in $Stx3^{\Delta/\Delta}$ MCs were ≤12 fF compared with ~35% in $Stx3^{F/F}$ MCs. In absolute numbers, the number of steps ≤8 fF in recordings from Stx3-deficient MCs (41 ± 7; mean ± S.E.; $n = 36$ cells from 8 animals) was very close to what we found in Stx3-sufficient MCs (35 ± 6; $n = 36$ cells from 6 animals; $p = 0.5$), whereas the numbers of events ≥40 fF were 4 ± 3 and 49 ± 11, respectively ($p < 0.001$).

The frequency distribution of step sizes was unaffected by the absence of Stx4 (Fig. 2*L*). We did not study the haploinsufficient $Stx4^{+/-}$ MCs in any experiment, given that full deficiency of Stx4 did not result in any electrophysiological abnormality. These results show that Stx3 is partially responsible for MC exocytosis and that the residual exocytosis after its deletion proceeds at a slower pace and is composed mainly of single-vesicle fusion events.

Absence of Stx3, but not Stx4, alters the ultrastructural changes associated with exocytosis in MCs

Measurement of C_m is blind to the intracellular events that take place during MC degranulation. Consequently, we studied EM profiles of peritoneal MCs stimulated with a combination of the diacylglycerol-analog phorbol 12-myristate 13-acetate (PMA) and the Ca^{2+} ionophore ionomycin. Qualitatively, stimulated Stx3-deficient MCs did not undergo the same amount of exocytosis as stimulated Stx3-sufficient MCs (Fig. 3*A*), whereas Stx4-sufficient or -deficient MCs were indistinguishable (Fig. 3*B*). To quantify those alterations, we studied cell profiles using stereology and also measured the electron lucency of the MC granules. When MCs are activated, they lose the electron den-

sity of their granules secondary to hydration and loss of granule contents (47, 48), and we quantified this change as gain in electron lucency (20). Compared with unstimulated controls, stimulated $Stx3^{+/+}$ MCs have a significant increase in electron lucency of their granules (right shift), whereas the signal from stimulated $Stx3^{\Delta/\Delta}$ MCs was intermediate between those two groups (Fig. 3*C*). On the other hand, the response to activation was indistinguishable between $Stx4^{\Delta/\Delta}$ and $Stx4^{+/+}$ MCs (Fig. 3*F*). The loss of electron-dense granules during degranulation can be quantified as the fraction of cytoplasm occupied by dense granules (volume density (*Vv*)) (49, 50). Once again, stimulated Stx3-deficient MCs behaved more like naive Stx3-sufficient MCs than stimulated Stx3-sufficient MCs (Fig. 3*D*), whereas the presence or absence of Stx4 made no difference (Fig. 3*G*).

The most remarkable morphological alteration in Stx3-deficient MCs was the almost complete absence of intracellular multigranular compartments after stimulation. In fact, this is the only measurement in which we found a partial defect in haploinsufficient $Stx3^{+/-}$ MCs (Fig. 3*E*). Deletion of Stx4 had no effect on this structural outcome (Fig. 3*H*). Because of the absence of a phenotype in Stx4-deficient MCs, $Stx4^{+/-}$ MCs were not studied. Altogether, these data suggest that although only a fraction of total MC exocytosis depends on Stx3, almost all MC compound exocytosis requires this protein.

Absence of Stx3, but not Stx4, affects selectively MC-regulated exocytosis

We wanted to address whether the defective MC degranulation we observed in Stx3-deficient MCs was linked to abnormalities in other MC effector responses and whether Stx4 was important for any MC secretory response at all. We measured the secretion of products that depend on regulated exocytosis, constitutive exocytosis, and nonexocytic transport (19, 20). PCMCs were stimulated via FcεRI or with PMA/ionomycin (PI). We quantified the amount of histamine and the fraction of total cell β-hexosaminidase secreted after stimulation. These two compounds are preformed, are stored in MC secretory granules, and are secreted via regulated exocytosis. To address constitutive exocytosis of newly synthesized cytokines, we measured the secretion of TNFα and IL4, and for responses independent of exocytosis, we measured the secretion of PGD_2 and LTC_4. Given that we had not detected any differences between $Stx4^{+/+}$ and $Stx4^{F/F}$ mice in all previous experiments, we included only $Stx4^{F/F}$ and $Stx4^{\Delta/\Delta}$ mice in this section.

In the β-hexosaminidase secretion assay, we detected the expected bell-shaped response curve to increasing amounts of antigen (19, 20, 22) in Stx3-sufficient PCMCs. Haploinsufficiency or homozygosity for the "floxed" allele of Stx3 did not affect this response, whereas Stx3 deficiency significantly impaired β-hexosaminidase release (Fig. 4, *A* and *C*). This defect was corrected once we used PI as a stronger stimulus (Fig. 4*C*). The defect in secretion of MC mediators released by regulated exocytosis and its correction under strong stimuli were confirmed when we measured histamine release in MCs activated via IgE-FcεRI (Fig. 4*D*) and PI (Fig. 4*E*). Despite that, the secretion of mediators released by constitutive exocytosis (Fig. 4, *F* and *G*) or transmembrane transporters (Fig. 4, *H* and *I*) was not affected by the deletion of Stx3. TNFα, IL4, PGD_2, and LTC_4 were undetectable in supernatants of unstimulated cells (not shown).

Independent of the mediator measured or the stimuli employed, we could not detect any secretory abnormality induced by the removal of Stx4 (Fig. 4, *B–I*). Because we did not detect any differences between Stx4-deficient and Stx4-sufficient MCs in any of the electrophysiology, EM, and secretion assays, we did not perform any *in vivo* experiments with the Stx4 mutant animals.

Stx3 deficiency does not affect MC numbers, distribution, differentiation, or structure

Defective exocytosis could also be caused by morphological or developmental anomalies in MCs (*e.g.* improper granule biogenesis or failure to exteriorize surface receptors) (51, 52). We studied MCs from all Stx3 mutant mice (Fig. 5 and Table 1). We found almost identical densities of dermal MCs and similar fractions, numbers, and metachromasia of MCs in peritoneal lavages. Flow cytometry assays showed a similar fraction of $CD117^+/Fc\epsilon RI\alpha^+$ double-positive cells in peritoneal lavages and in PCMCs after 2 weeks in medium enriched with IL3 and stem cell factor. In these two assays, the fluorescence intensity for CD117 and FcεRIα in nonpermeabilized cells is proportional to the surface expression of these two receptors, and they were unchanged. Stereology of EM MC profiles revealed similar cell surface density (*Sv* cell) and cell profile area in all genotypes, indicating that the surface complexity, size, and shape of the cell profiles were not affected. Also, the fact that both *Vv* granule and *Sv* granule were similar indicates that there were no changes in the number, size, and shape of the MC granules. All of these parameters were also unchanged in $Stx4^{+/+}$, $Stx4^{+/-}$, $Stx4^{F/F}$, and $Stx4^{\Delta/\Delta}$ mice (not shown).

Therefore, the changes in the preceding *ex vivo* assays cannot be explained by a structural abnormality in the absence of Stx3, and any phenotype detected in subsequent *in vivo* experiments cannot be attributed to changes in the number or distribution of MCs in the mutant mice.

Stx3 deficiency does not alter MC-dependent anaphylactic responses

We have shown in mice with defective MC exocytosis that there is a correlation between the severity of the exocytic defect and protection in a model of passive systemic anaphylaxis (20, 22). In this model, the degree of core body heat loss is proportional to the severity of the anaphylaxis (53–55). The lack of response in MC-deficient (Wsh) mice confirmed the MC dependence of this reaction (Fig. 6*A*, *gray line*), and the antigen challenge by itself did not induce hypothermia (Fig. 6*A*, *black line*). We found no differences in the hypothermic response among all Stx3 genotypes (Fig. 6, *A* and *B*), despite histologic evidence that degranulation of $Stx3^{\Delta/\Delta}$ MC in connective tissues was partially deficient (Fig. 6, *C* and *D*).

Discussion

The Stx responsible for MC degranulation was originally identified as Stx4 (23, 24). Paumet *et al.* reported that overexpression of Stx4 decreased FcεRI-dependent degranulation in

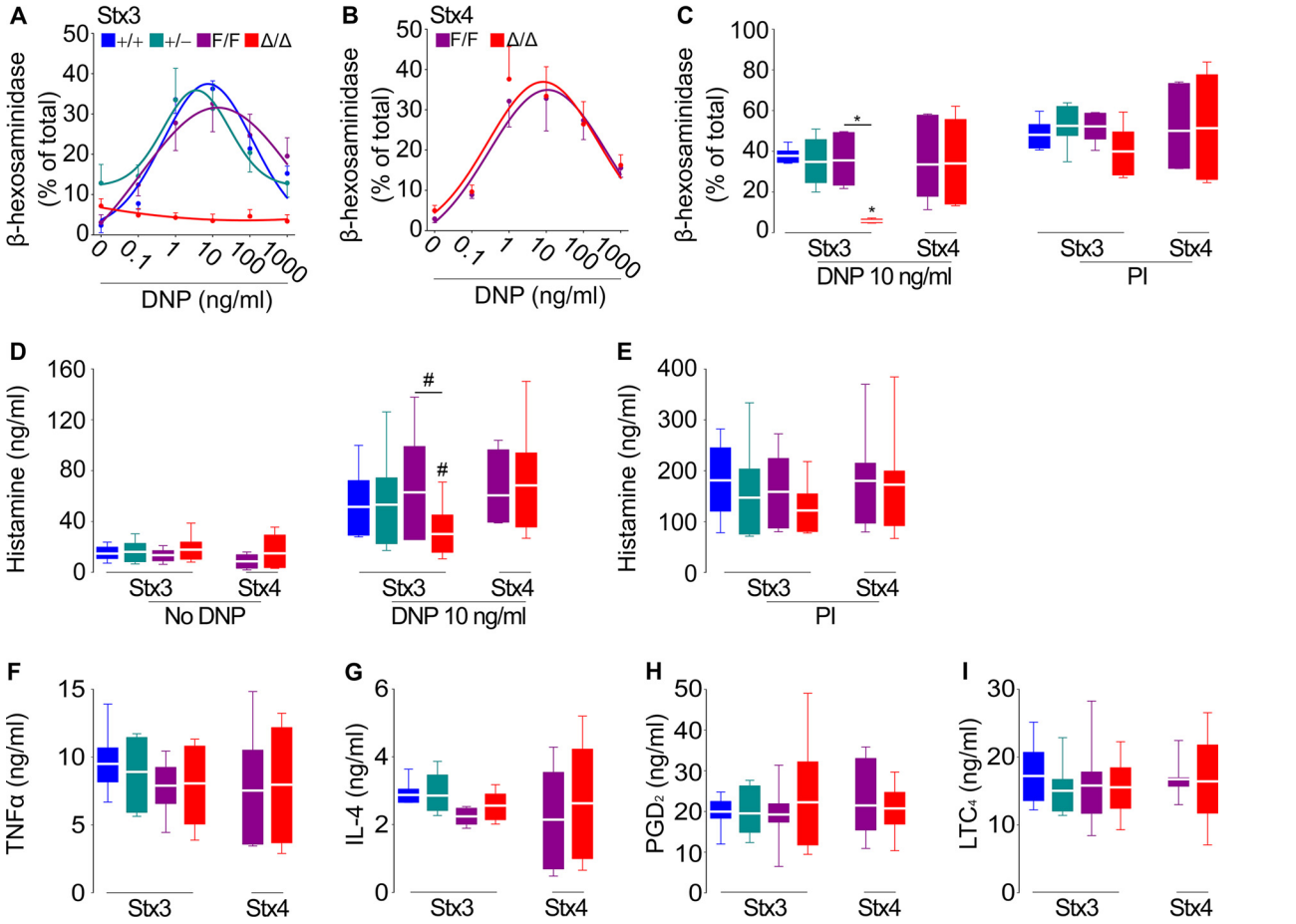

Figure 4. Absence of Stx3, but not Stx4, alters mainly regulated exocytosis in MCs. PCMCs were sensitized with anti-DNP IgE and then challenged with DNP-HSA (*DNP*) or PI. The *color key* in *A* and *B* applies to *all panels*. Regulated exocytosis was monitored by measuring the fraction of total cell β-hexosaminidase (*A–C*) and the amount of histamine (*D* and *E*) secreted 30 min post-stimulation with PI. Constitutive exocytosis was monitored by measuring secretion of TNFα (*F*) and IL4 (*G*) 6 h post-stimulation with PI. Secretion independent of exocytosis was monitored by measuring PGD_2 (*H*) and LTC_4 (*I*) 30 min post-stimulation. *n* = cells derived from 7–8 mice of each genotype; *circle* and *white line*, mean; *error bar*, S.E.; *box*, 25th–75th percentile; *whiskers*, 5th–95th percentile. #, $p \leq 0.05$; *, $p \leq 0.001$; all compared with +/+ PCMCs unless otherwise specified.

RBL-2H3 cells (25). Then Stx4 was shown to form SNARE complexes with SNAP23 in RBL-2H3 cells (25, 26, 29, 56), mouse bone marrow–derived MCs (BMMCs) (57), and human intestine-derived MCs (31). In this last study, Sander *et al.* (31) found that treatment of permeabilized cells with anti-Stx4 antibodies decreased significantly their release of histamine after stimulation via FcεRI or with PI (31). A similar experiment was performed by Salinas *et al.* (30) in permeabilized rat peritoneal MCs. They found that incubation with anti-Stx4 antibodies diminished histamine secretion induced by exposure to Ca^{2+} and GTPγS (30). Woska *et al.* knocked down Stx4 expression in RBL-2H3 cells using siRNAs and observed a significant reduction in IgE-dependent β-hexosaminidase release (27). Also, using an Stx4 siRNA in RBL-2H3 cells, Liu *et al.* (28) showed that reductions in Stx4 expression induced impairments in IgE- and thapsigargin-dependent release of histamine and β-hexosaminidase, but not of IL4 and LTC_4. More recently, Yang *et al.* (58) showed that a synthetic peptide based on the N terminus of Stx4 was able to inhibit lipid mixing in a liposome fusion assay that used the SNAREs Stx4, SNAP23, and VAMP2 or -8. The same Stx4 peptide inhibited degranulation when introduced into RBL-2H3 cells (58). Here we studied fully mature MCs in which expression of Stx4 was not partially, but completely, eliminated (Fig. 1).

We assessed exocytosis using three different methods, two of them extremely sensitive (C_m measurements and EM). We also activated these MCs using FcεRI-dependent, and receptor-independent (PI and Ca^{2+}-GTPγS), pathways. Despite all that, we found no abnormalities in exocytosis in Stx4-deficient MCs, whether single-vesicle or compound, regulated or constitutive (Figs. 2–4). These findings correlate with our previous observation that in the absence of Munc18-3, perhaps the exclusive functional partner of Stx4 (59–61), MC exocytosis was normal (22). Thus, Stx4 could be added to the list of exocytic proteins (including synaptotagmin-2 and Munc18-1) in which there is a poor correlation between findings in cell lines and mature MCs. Another factor that could explain our disagreement with previous reports is that we used deletion of Stx4 instead of relying on antibodies, peptides, or siRNAs, all of which could have significant off-target effects on other Stxs or proteins that interact with them. Finally, our results suggest that efforts to target Stx4 expression or function to therapeutically control pathologic manifestations precipitated by MC degranulation (28, 58) ought to be viewed with high skepticism.

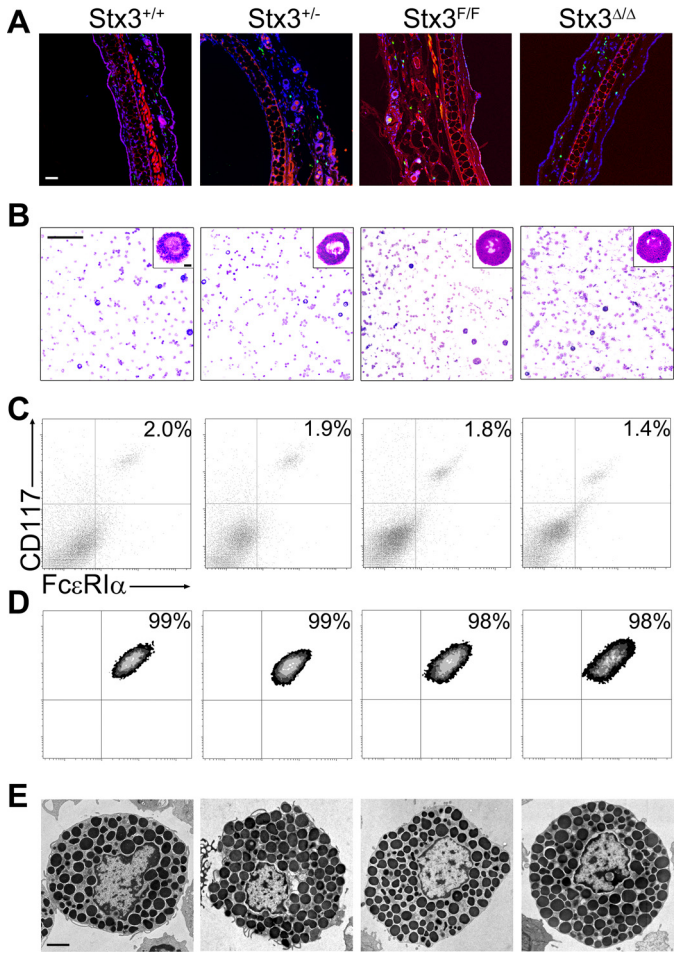

Figure 5. Absence of Stx3 does not affect the total number, distribution or structure of MCs. Shown are representative images; for detailed quantification, please refer to Table 1. *A*, ear sections stained with FITC-avidin (*green*) and Hoechst (*blue*); autofluorescence in the red channel delimited the dermis. *Scale bar*, 50 μm. *B*, cytospins of peritoneal MCs stained with Wright–Giemsa. *Scale bar*, 200 μm; *inset scale bar*, 50 μm. Flow cytometry of peritoneal MCs (*C*) and PCMCs (*D*) labeled with antibodies against CD117 and FcεRIα. *E*, EM profiles of resting peritoneal MCs. *Scale bar*, 2 μm.

Table 1
Characterization of MCs from mutant Stx3 mice

Results are mean ± S.E. from six mice of each genotype. A, cell profile area; AU, arbitrary units; MFI, mean fluorescence intensity. No significant differences were found among mice of all genotypes in any category.

	$Stx3^{+/+}$	$Stx3^{+/-}$	$Stx3^{F/F}$	$Stx3^{\Delta/\Delta}$
Dermal MCs				
Density (cells/mm^2 of dermis)[a]	123 ± 10	108 ± 9	98 ± 10	103 ± 9
Peritoneal MCs				
Count (cells/μl)[b]	19 ± 5	16 ± 4	18 ± 2	22 ± 6
MCs (%)[b]	2.0 ± 0.4	1.8 ± 0.5	1.9 ± 1.0	2.1 ± 0.8
Vv[c]	0.65 ± 0.10	0.59 ± 0.10	0.68 ± 0.12	0.66 ± 0.11
Sv cell (μm^{-1})[c]	0.69 ± 0.18	0.64 ± 0.17	0.66 ± 0.18	0.74 ± 0.17
Sv granule (μm^{-1})[c]	4.70 ± 0.56	4.98 ± 0.69	4.58 ± 0.61	4.37 ± 0.57
A (μm^2)[c]	78.9 ± 12.4	77.7 ± 11.7	63.2 ± 11.9	71.7 ± 15.0
$CD117^+/FcεRIα^+$ (%)[d]	2.1 ± 0.3	1.9 ± 0.5	1.8 ± 0.8	1.7 ± 0.1
MFI CD117 (AU)[e]	12.5 ± 8.7	13.9 ± 6.3	12.9 ± 2.2	13.2 ± 7.8
MFI FcεRIα (AU)[e]	2.9 ± 0.4	3.2 ± 0.6	3.1 ± 0.1	2.9 ± 0.7
PCMCs				
$CD117^+$, $FcεRIα^+$ (%)[d]	98.1 ± 0.1	97.6 ± 0.1	99.0 ± 0.2	96.9 ± 0.1
MFI CD117 (AU)[e]	9.0 ± 0.2	9.2 ± 0.2	9.1 ± 0.2	8.9 ± 0.3
MFI FcεRIα (AU)[e]	6.6 ± 0.7	7.0 ± 0.6	6.4 ± 0.6	7.1 ± 0.5

[a] Cells with FITC-avidin$^+$ granules and a Hoechst$^+$ nucleus per mm^2 of dermis in random 5-μm sections of ear (10 sections/mouse).
[b] Neubauer chamber counts and differentials of cytospins of recovered peritoneal lavage (1 sample/mouse).
[c] Stereological analysis of randomly acquired EM images of peritoneal MCs (30 cell profiles/mouse).
[d] Fraction of $CD117^+/FcεRIα^+$ cells in peritoneal MCs or PCMCs assessed by flow cytometry (1 sample/mouse).
[e] Cell surface expression of CD117 and FcεRIα expressed as mean fluorescence intensity of labeled specific primary antibodies (1 sample/mouse).

Although overexpression of Stx3 in RBL-2H3 cells did not affect degranulation (25), treatment of permeabilized human intestine-derived MCs with anti-Stx3 antibodies inhibited the stimulated release of chemokines (40). Others found that partial knockdown of Stx3 in RBL-2H3 cells and mouse BMMCs hindered degranulation but not chemokine secretion (37, 38). In RBL-2H3 cells, the effects of Stx3 on degranulation depended on a specific interaction with Munc18-2 (38, 39).

We removed expression of Stx3 in mature MCs (Fig. 1*B*). Based on our previous finding that deletion of Munc18-2 in fully developed MCs eliminated MC degranulation almost completely (22) and the proven physical and functional interaction between Munc18-2 and Stx3 in cultured cells (37, 38), we were expecting a similarly severe exocytic defect in $Stx3^{\Delta/\Delta}$ MCs. Applying the high sensitivity of C_m measurements to peritoneal MCs, we identified a significant reduction in stimulated MC exocytosis. Nonetheless, despite what the results in cultured cells suggested, the defect in Stx3-deficient MCs was not absolute, as we recorded ~40% of residual exocytosis in Stx3-deficient MCs (Fig. 2*B*). The difference in exocytic failure between our Munc18-2–deficient and Stx3-deficient MCs indicates that another Stx should also mediate this process. We have now shown definitely that it is not Stx4. Stx1a and Stx1b function almost exclusively in neurons, and we have been unable to detect their expression by immunoblots in mature MCs (not shown). We speculate that, among the Stxs known to interact with Munc18-2, Stx2 and Stx11 are the best candidates to explain the residual exocytosis. In other immune cells, Stx3 and Stx11 are redundant to each other in mediating Munc18-2–dependent exocytosis (62). In MCs, the effects of Stx2 or Stx11 deficiency on exocytosis have not been studied at high resolution yet.

The residual exocytosis we recorded in MCs lacking Stx3 happened at a markedly slower rate compared with controls (Fig. 2*D*). It has been postulated that one mechanism used by MCs to accelerate exocytosis is compound exocytosis (63). Sequential compound exocytosis shortens the distance (and thus the time required for fusion) between granule and target membrane, and multigranular compound exocytosis allows the content from multiple granules to be released in a single fusion event with the plasma membrane (11). It is estimated that the membrane from a single MC granule would increase C_m by ~7 fF (64). When we measured the contribution of single-capacitance steps to ΔC_m, we found that MCs from $Stx3^{\Delta/\Delta}$ mice had a clear deviation toward small steps, whereas large steps were almost completely absent (Fig. 2*K*). These findings had a perfect correlate in our morphologic studies, in which we observed that activated $Stx3^{\Delta/\Delta}$ MCs had only a partial defect in quantitative EM markers of exocytosis (Fig. 3, *C* and *D*), whereas there was virtually an absence of multigranular compartments (Fig. 3*E*). There was also a close correlation between the only two manifestations of haploinsufficiency in $Stx3^{+/-}$ MCs; a decrease in

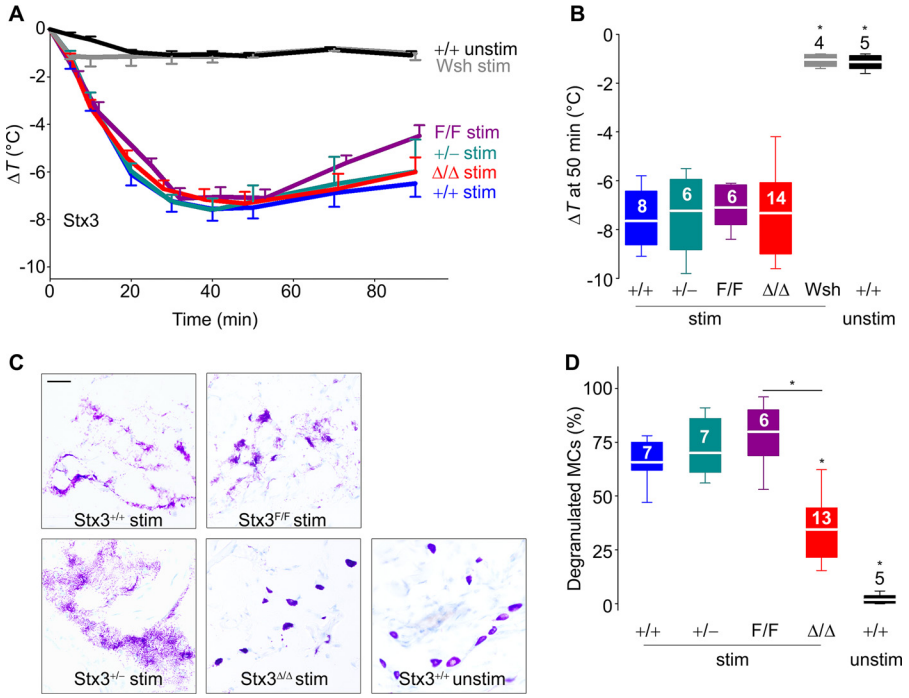

Figure 6. Absence of Stx3 does not interfere with MC-dependent anaphylactic responses. MC-deficient Kit$^{W\text{-}sh/W\text{-}sh}$ (Wsh) and Stx3 mutant mice were sensitized i.p. with anti-DNP IgE and challenged i.p. with DNP-HSA (*stim*) or vehicle only (*unstim*). *A*, changes in body core temperature (ΔT) post-challenge. *B*, ΔT at 50 min post-challenge. *Number inside boxes* in *B*, number of animals; applies to *A* and *B*. *C*, representative lip sections 90 min post-challenge stained with toluidine blue. *Scale bar*, 5 μm. *D*, fraction of degranulated MCs in lip sections. *Number inside boxes*, number of animals. *White line*, mean; *box*, 25th–75th percentile; *whiskers*, 5th–95th percentile. *, $p < 0.001$; all compared with +/+ stimulated MCs unless otherwise specified.

the *Vv* of compound compartments (Fig. 3*E*) was associated with slower kinetics of exocytosis (Fig. 2*D*). These results confirm that the long-held hypothesis that MCs use compound exocytosis to accelerate their rate of exocytosis (10) is correct.

The possible role of Stx3 in granule-to-granule fusion was suggested by its localization on the granule membrane (34–36, 57). Here, we show that removal of Stx3 results in a nearly complete failure of this process. The severe defect in MC compound exocytosis is not unique to the absence of Stx3. We have seen the same in MCs deficient in Munc18-2 (22) and Munc13-4 (20). Thus, it seems that the homotypic fusion step of multigranular compound exocytosis requires Stx3, Munc13-4, and Munc18-2.

On the other hand, whereas deletion of Munc18-2 removed almost all traces of single-vesicle exocytosis as well as compound exocytosis, removal of Munc13-4 and Stx3 left a residual response composed almost entirely of single-vesicle fusion events. In the case of Munc13-4, the additional deletion of Munc13-2 eliminated the remaining exocytosis (20). For Stx3, the number of steps reflecting single-vesicle exocytosis (≤8 fF) was similar between Stx3-deficient and Stx3-sufficient MCs, but fusion of single vesicles alone was insufficient to achieve normal levels of total exocytosis, even at a slower rate. Therefore, the heterotypic fusion between granule membrane and plasma membrane requires mainly Munc18-2 and Munc13-4 and probably an Stx other than Stx3. Moreover, we show for the first time that the importance of compound exocytosis in MCs is not only to help achieve faster secretory kinetics, but also that it is required for full degranulation (Fig. 2).

Although we saw a severe impairment in compound exocytosis in the absence of Munc18-2, the effects of removing Stx3 on this process are not indirectly due to alterations in the expression of Munc18-2 (Fig. S2). The lack of an effect of absence of Stx3 on Munc18-2 expression could be due to the presence of other Munc18-2–interacting Stxs in MCs. For example, in cytotoxic T-lymphocytes, disruption of expression of Stx11 does not alter expression of Munc18-2 (65). On the other hand, the fact that removing Stx3 affects compound but not single-vesicle exocytosis, whereas deleting Munc18-2 affects both, mitigates against the possibility that all of the effects of Munc18-2 are mediated by Stx3.

Similar to what we observed after removing synaptotagmin-2 (19) and Munc13-4 (20), Stx3 deficiency affected mainly regulated exocytosis, leaving other responses intact, including constitutive exocytosis (Fig. 4). This makes sense, given that compound exocytosis has been described as a mechanism in regulated exocytosis but not in constitutive exocytosis (66). The normal secretion of PGD_2 and LTC_4 obtained from Stx3$^{\Delta/\Delta}$ MCs confirms that these cells can be stimulated and rules out faulty activation as an explanation for the secretory defect. The secretion of histamine and β-hexosaminidase was reduced in Stx3-deficient MCs as we observed in Munc13-4– and Munc18-2–deficient MCs (20, 22), but unlike in the MCs from the two mutants, the secretion of these two mediators was rescued in Stx3-deficient MCs by using a stronger stimulus (Fig. 4). This correlates perfectly with the fact that the defects observed in ΔC_m (Fig. 2) and EM stereology (Fig. 3) in MCs lacking Stx3 were also only partial, whereas those we reported in the absence of Munc13-4 (20) and Munc18-2 (22) were almost complete, demonstrating once again the complementarity of electrophysiology, stereology, and secretion assays in MCs.

The defective exocytosis we recorded in Stx3$^{\Delta/\Delta}$ MCs had no impact on the development and distribution of MCs in the mutant animals (Fig. 5 and Table 1). This allowed us to proceed with whole-animal experiments. The partial exocytic defect we identified in isolated Stx3-deficient MCs tightly correlated with the histologic assessment of MC degranulation in Stx3$^{\Delta/\Delta}$ mice subjected to a model of systemic anaphylaxis (Fig. 6, *C* and *D*). Despite that, this partial defect did not affect the hypothermic response, our main outcome (Fig. 6, *A* and *B*). This agrees with our findings on Munc13-4 and Munc18-2 mutant mice in which only an absolute deficiency in MC exocytosis had an impact on anaphylaxis outcome, whereas partial defects in expression had no effects on this allergic response (20, 22).

Experimental procedures

Mice

We purchased B6 (catalogue no. 000664), MC-deficient B6.Cg-*Kit*$^{W\text{-}sh}$/HNihrJaeBsmGlliJ (Wsh/Wsh; catalogue no. 012861), B6.129S4-*Gt(ROSA)26Sor*$^{tm1(FLP1)Dym}$/RainJ (catalogue no. 009086), and B6.C-Tg(CMV-cre)1Cgn/J mice (catalogue no. 006054) from the Jackson Laboratory. We obtained Tg(Cma1-cre)ARoer mice from Dr. Axel Roers (University of Cologne) (67).

To generate Stx3 cKO mice, we obtained ES cells from EUCOMM (clone EUCE320f12). These 129/Ola ES cells contain a gene trap flanked by inversely oriented pairs of the heterotypic FRT/F3 and lox511/loxP recombinase target sequences (68). The cassette, located in intron 1 of the *Stx3* gene (GRCm38; Chr19:1806110) includes the following, from 5′ to 3′: a long terminal repeat, an FRT, an F3, a loxP, a lox511, a splice acceptor, β-gal/neomycin phosphotransferase fusion gene, a polyadenylation site, a loxP, a lox511, an FRT, and an F3. The mechanism relies on two-directional site-specific recombination systems: FLPe/FRT and Cre/loxP. The former inverts the gene trap from its sense (mutagenic) orientation to antisense, allowing expression of Stx3 (F allele); the latter reinduces the mutation by the reinversion of gene trap to its sense orientation, stopping expression of Stx3 (Δ and − alleles). We injected the ES cells into B6 blastocysts, established a line, and backcrossed it into B6 until all 105 SNPs from a speed-congenic scanning confirmed a pure B6 background. Using FLPe-mediated recombination by crossings with B6.129S4-*Gt(ROSA)26Sor*$^{tm1(FLP1)Dym}$/RainJ mice, we recovered Stx3 expression (Stx3$^{F/F}$), leaving the allele susceptible to future inactivation via Cre recombinase.

To create an Stx4 cKO, we engineered a targeting vector to insert a loxP upstream of exon 1 (GRCm38; Chr7:127841278) of the mouse *Stx4* gene by homologous recombination. A second loxP site, followed by the phosphoglucokinase promoter-driven neomycin resistance gene (PGK-Neo) flanked by two FRT sites, was introduced in intron 4 (GRCm38; Chr7:127842997). The herpes simplex virus thymidine kinase gene was introduced outside the homology region. The construct was electroporated into B6 ES cells, and mutant mice were produced and selected as described (20). We crossed mice with confirmed germ line transmission of the mutant Stx4 allele with B6.129S4-*Gt(ROSA)26Sor*$^{tm1(FLP1)Dym}$/RainJ mice to remove PGK-Neo and leave exons 1–4 susceptible to Cre recombination (F allele).

In both cases, we obtained MC-specific deletion (Stx3$^{\Delta/\Delta}$ and Stx4$^{\Delta/\Delta}$) by crossing the respective F/F mice with Tg(Cma1-cre)ARoer mice, which express Cre recombinase under the control of the *Cma1* locus, a protease expressed exclusively in MCs (67). We also obtained germ line/global/constitutional heterozygous deletion (Stx3$^{+/-}$ and Stx4$^{+/-}$) by crossing F/F mice with B6.C-Tg(CMV-cre)1Cgn/J mice and crossing the products with B6 mice to confirm germ line deletion before stablishing the lines (69). Genotyping was done using PCR. For Stx3, we used the following primers: 1) 5′-GCAGACAGACATGGTGTTGG-3′, 2) 5′-CCCTTTCCTTTCCTGAGCC-3′, and 3) 5′-GGAAACCCTGGACTACTGCG-3′, which produced distinct bands for the + allele (461 bp), F allele (2057 bp), and − allele (890 bp). For Stx4, we used the primers 1) 5′-CCGAATTTGGTGTTGGGATT-3′, 2) 5′-CAGGTCACACAGCAGACTTGGG-3′, and 3) 5′-TGGATCTCCGTGCATTTGAGG-3′ to differentiate the + allele (405 bp) from the F allele (473 bp) and the − allele (678 bp).

We used littermates as controls in all experiments and included adult animals of both sexes. All studies were carried out using animal protocols approved by the Institutional Animal Care and Use Committee of the University of Texas M.D. Anderson Cancer Center.

MC harvesting, cultures, secretion assays, flow cytometry, and cell sorting

After euthanasia, we lavaged the peritoneal cavity as described (70). We counted cells in a Neubauer chamber and cytospins stained with Wright–Giemsa and toluidine blue (pH 0.5). The peritoneal lavage cells were washed with PBS and processed for different assays. For PCMCs, we resuspended the cells in medium supplemented with rmIL-3 (5 ng/ml) and stem cell factor (15 ng/ml; both from R&D Systems) and cultured them for 2 weeks (37 °C, 5% CO_2) with biweekly medium exchanges. For secretion assays, 3×10^4 PCMCs were incubated for 5 h with 100 ng/ml SPE-7 anti-DNP IgE (Sigma-Aldrich), washed, and stimulated with DNP-HSA or PMA/ionomycin to assess secretion of β-hexosaminidase, histamine, LTC_4, and PGD_2 at 30 min, and of TNFα and IL4 at 6 h as described (20, 22). For flow cytometry, we incubated peritoneal MCs and PCMCs with 200 ng of anti-mouse CD117 phycoerythrin-cyanine-7 and 200 ng of anti-mouse FcεRIα Alexa Fluor 647 (both from eBioscience) in 100 μl of PBS at room temperature for 25 min, washed them in PBS twice, and then analyzed them (LSRII; BD Biosciences), recording the number of CD117$^+$/FcεRIα$^+$ cells and their mean fluorescence intensity. For sorting, we labeled the cells as above and collected the CD117$^+$/FcεRIα$^+$ double-positive cells (BD FACSAria).

Expression studies

For RT-qPCR, we extracted RNA (RNeasy mini kit; Qiagen) from FACS-sorted peritoneal MCs and reverse-transcribed it (qSCRIPT cDNA SuperMix; Quantabio). We used FAM-labeled probes for β-actin (Mm02619580_g1), Stx1a (Mm00444008_m1), Stx1b (Mm01275274_m1), Stx2 (Mm04229900_m1), Stx3 (Mm01197689_m1), Stx4 (Mm00436827_m1), and

Stx11 (Mm01192495_m1) (all from Thermo Fisher Scientific). Quantitative PCR of each cDNA sample was obtained in triplicates (ViiA 7 RT-PCR system; Applied Biosystems). All of the results were expressed as $\Delta\Delta Ct$ (normalized for β-actin and then for levels in WT controls). For immunoblots, we homogenized and sonicated mouse tissues and PCMCs in cell lysis buffer with protease inhibitors (Sigma-Aldrich). We ran the lysates under denaturing conditions in 10% SDS-polyacrylamide gels and transferred them to nitrocellulose membranes (Bio-Rad). Blots were probed with anti-Stx3 (1:1000; ab133750; Abcam), anti-Stx4 (1:750; S9924; Sigma-Aldrich), anti-Munc18–2 (1:200; HPA015564; Sigma-Aldrich), and anti-β-actin (1:30,000; ab119716; Abcam) antibodies.

Histology

We harvested ears and lips and fixed them in 4% paraformaldehyde (pH 7.0) overnight at 4 °C and processed for histology. Paraffin-embedded 5-μm sections were labeled with 1:1000 FITC-avidin and 1:10,000 Hoechst 33342 (Molecular Probes, Life Technologies) (21). We identified MCs as Hoechst$^+$ nuclei surrounded by FITC-avidin$^+$ granules and identified the dermis as the area between the epidermis and the skeletal muscle or auricular cartilage and then reported the number of MCs per area of dermis (2). OCT-embedded 5-μm sections were stained with toluidine blue (pH 0.5), and we counted an MC as degranulated if >50% of its metachromatic granules were visualized outside the cell (22).

EM and stereology

We activated peritoneal MCs by resuspending peritoneal lavage cells in 1 ml of 300 nM PMA and 1.2 μM ionomycin in PBS. After 5 min, we stopped exocytosis and fixed the cells by adding 2 ml of cold buffered 2.5% glutaraldehyde on ice for 15 min; the fixation continued at room temperature for 2 h. Resting cells were fixed the same way. After washings in PBS, we resuspended the fixed cells in 0.1 M sodium cacodylate in PBS. The processing and imaging of the cells was done as described (2). We analyzed the images on STEPanizer (71). We used point counting to determine the *Vv* values of dense granules and multivesicular compound granules and used line intersections with plasma membrane and granule membranes to obtain *Sv* values (72). The relative electron lucency of MC granules was analyzed as described (20). In short, with a circle-cycloid stereological grid, random points were captured to generate a 0–255 linear gray scale unique to each image, and the digital grayness of circles with an area of 0.0366 μm^2 within randomly selected granules was compared against this scale. Granules with relative electron lucency of <120 were categorized as dense.

Electrophysiology

We obtained single-cell capacitance recordings as described before (20, 22) with slight variations. We resuspended peritoneal cells in external solution (137 mM NaCl, 2.6 mM KCl, 10 mM HEPES, 2 mM $CaCl_2$, 0.5 mM $MgCl_2$, 0.4 mM $MgSO_4$, 10 mM glucose, 0.44 mM KH_2PO_4, 0.34 mM Na_2HPO_4, pH 7.3, 0.310 osmol). Whole-cell recordings from individual MCs were made using 5–6-megaohm SYLGARD-coated patch pipettes. The internal solution (135 mM potassium gluconate, 10 mM HEPES, 7 mM $MgCl_2$, 3 mM KOH, 0.2 mM Na_2 ATP, 0.05 mM Li_4 GTPγS, 2.5 mM Cs_2-EGTA, 7.5 mM Ca-EGTA, 0.1 mM Fura-2, pH 7.21, 0.302 osmol) defined intracellular [Ca^{2+}] and induced degranulation. Cytoplasmic [Ca^{2+}] was measured ratiometrically with Fura-2, and Ca^{2+} calibration constants were determined *in vitro* using a multipoint calibration kit (Thermo Fisher Scientific/Molecular Probes) and analyzed in IgorPro (WaveMetrics). For recordings of membrane capacitance (C_m), membrane conductance (G_m) and series conductance (G_s), an 800-Hz sinusoidal, 30-mV peak-to-peak stimulus was applied around a holding potential of −70 mV, and the resultant signal was analyzed using the Lindau–Neher technique (73). For each 100-ms sweep, the average value was recorded, yielding a temporal resolution for C_m, G_m, and G_s of ~7 Hz. Cells selected for analysis met the criteria of $G_m \leq 1{,}200$ pS, $G_s \geq 35$ nS, and steady-state intracellular [Ca^{2+}] ~400 ± 100 nM. ΔC_m, rates of ΔC_m from 40 to 60% of total ΔC_m, time interval between cell access and exocytic burst, and size and number of C_m steps between 1 and 15% of total ΔC_m were obtained as described (22).

Passive systemic anaphylaxis

We sensitized 15–18-week-old mice with 10 μg of mouse anti-DNP IgE (SPE-7; Sigma-Aldrich) in 200 μl of PBS i.p. The next day, we challenged the mice with 500 μg of DNP-HSA in 200 μl of PBS i.p. We monitored the basal core body temperature over time with a rectal thermometer probe (Sper Scientific), euthanized the mice at 90 min, and harvested the lips for histology.

Statistical analysis

For continuous variables, we first tested for normality with D'Agostino's K2 test. For normal data, we first compared the means of all groups by analysis of variance, and if a significant difference was found, we applied Tukey's honest significant difference test for multiple pairwise comparisons, Dunnett's test for multiple comparisons against the control group, or Student's *t* test for single comparisons. For nonnormal data, we first compared all groups using a Kruskal–Wallis *H* test and followed any significant result with Dunn's test for multiple comparisons or the Mann–Whitney *U* test for single comparisons. For categorical data, we used Pearson's χ^2 test or Fisher's exact test. We analyzed frequency distributions with the Kolmogorov–Smirnov test. Significance was set at $p <$ 0.05.

Author contributions—E. S., D. S. M., M. A. C., B. A. G., and R. H. software; E. S., D. S. M., M. A. C., B. A. G., A. R. B., R. H., and R. A. formal analysis; E. S., E. A. G., D. S. M., R. A. C., M. A. R., A. J. D., J. M., A. I. R., Y. P., D. C. M., A. T., A. L., A. R. B., and R. A. investigation; E. S., E. A. G., D. S. M., R. A. C., M. A. R., A. J. D., J. M., A. I. R., Y. P., D. C. M., A. T., A. L., A. R. B., and R. A. methodology; E. A. G., A. R. B., and R. A. visualization; A. R. B., R. H., and R. A. supervision; R. H. and R. A. data curation; R. A. conceptualization; R. A. resources; R. A. funding acquisition; R. A. validation; R. A. writing-original draft; R. A. project administration; R. A. writing-review and editing.

Acknowledgments—We thank Evelyn S. Brown and Margaret Gondo (University of Houston) for professional assistance with EM, Dr. Thomas C. Südhof for the backbone of the targeting vector for Stx4, and Dr. Axel Roers for the Tg(Cma1-cre)ARoer mouse line.

References

1. Galli, S. J., and Tsai, M. (2010) Mast cells in allergy and infection: versatile effector and regulatory cells in innate and adaptive immunity. *Eur. J. Immunol.* **40,** 1843–1851 CrossRef Medline
2. Thakurdas, S. M., Melicoff, E., Sansores-Garcia, L., Moreira, D. C., Petrova, Y., Stevens, R. L., and Adachi, R. (2007) The mast cell-restricted tryptase mMCP-6 has a critical immunoprotective role in bacterial infections. *J. Biol. Chem.* **282,** 20809–20815 CrossRef Medline
3. Stevens, R. L., and Adachi, R. (2007) Protease-proteoglycan complexes of mouse and human mast cells and importance of their β-tryptase-heparin complexes in inflammation and innate immunity. *Immunol. Rev.* **217,** 155–167 CrossRef Medline
4. Metcalfe, D. D., Baram, D., and Mekori, Y. A. (1997) Mast cells. *Physiol. Rev.* **77,** 1033–1079 CrossRef Medline
5. Blank, U., and Rivera, J. (2004) The ins and outs of IgE-dependent mast-cell exocytosis. *Trends Immunol.* **25,** 266–273 CrossRef Medline
6. Gilfillan, A. M., and Beaven, M. A. (2011) Regulation of mast cell responses in health and disease. *Crit. Rev. Immunol.* **31,** 475–529 CrossRef Medline
7. Galli, S. J., Kalesnikoff, J., Grimbaldeston, M. A., Piliponsky, A. M., Williams, C. M., and Tsai, M. (2005) Mast cells as "tunable" effector and immunoregulatory cells: recent advances. *Annu. Rev. Immunol.* **23,** 749–786 CrossRef Medline
8. Burgoyne, R. D., and Morgan, A. (2003) Secretory granule exocytosis. *Physiol. Rev.* **83,** 581–632 CrossRef Medline
9. Oberhauser, A. F., and Fernandez, J. M. (1996) A fusion pore phenotype in mast cells of the ruby-eye mouse. *Proc. Natl. Acad. Sci. U.S.A.* **93,** 14349–14354 CrossRef Medline
10. Alvarez de Toledo, G., and Fernandez, J. M. (1990) Compound *versus* multigranular exocytosis in peritoneal mast cells. *J. Gen. Physiol.* **95,** 397–409 CrossRef Medline
11. Pickett, J. A., and Edwardson, J. M. (2006) Compound exocytosis: mechanisms and functional significance. *Traffic* **7,** 109–116 CrossRef Medline
12. Burgess, T. L., and Kelly, R. B. (1987) Constitutive and regulated secretion of proteins. *Annu. Rev. Cell Biol.* **3,** 243–293 CrossRef Medline
13. Boyce, J. A. (2005) Eicosanoid mediators of mast cells: receptors, regulation of synthesis, and pathobiologic implications. *Chem. Immunol. Allergy* **87,** 59–79 Medline
14. Weber, T., Zemelman, B. V., McNew, J. A., Westermann, B., Gmachl, M., Parlati, F., Söllner, T. H., and Rothman, J. E. (1998) SNAREpins: minimal machinery for membrane fusion. *Cell* **92,** 759–772 CrossRef Medline
15. Teng, F. Y., Wang, Y., and Tang, B. L. (2001) The syntaxins. *Genome Biol.* **2,** REVIEWS3012 Medline
16. Ye, S., Karim, Z. A., Al Hawas, R., Pessin, J. E., Filipovich, A. H., and Whiteheart, S. W. (2012) Syntaxin-11, but not syntaxin-2 or syntaxin-4, is required for platelet secretion. *Blood* **120,** 2484–2492 CrossRef Medline
17. Chen, Y. A., and Scheller, R. H. (2001) SNARE-mediated membrane fusion. *Nat. Rev. Mol. Cell Biol.* **2,** 98–106 CrossRef Medline
18. Südhof, T. C. (2013) Neurotransmitter release: the last millisecond in the life of a synaptic vesicle. *Neuron* **80,** 675–690 CrossRef Medline
19. Melicoff, E., Sansores-Garcia, L., Gomez, A., Moreira, D. C., Datta, P., Thakur, P., Petrova, Y., Siddiqi, T., Murthy, J. N., Dickey, B. F., Heidelberger, R., and Adachi, R. (2009) Synaptotagmin-2 controls regulated exocytosis but not other secretory responses of mast cells. *J. Biol. Chem.* **284,** 19445–19451 CrossRef Medline
20. Rodarte, E. M., Ramos, M. A., Davalos, A. J., Moreira, D. C., Moreno, D. S., Cardenas, E. I., Rodarte, A. I., Petrova, Y., Molina, S., Rendon, L. E., Sanchez, E., Breaux, K., Tortoriello, A., Manllo, J., Gonzalez, E. A., *et al.* (2018) Munc13 proteins control regulated exocytosis in mast cells. *J. Biol. Chem.* **293,** 345–358 CrossRef Medline
21. Kim, K., Petrova, Y. M., Scott, B. L., Nigam, R., Agrawal, A., Evans, C. M., Azzegagh, Z., Gomez, A., Rodarte, E. M., Olkkonen, V. M., Bagirzadeh, R., Piccotti, L., Ren, B., Yoon, J. H., McNew, J. A., *et al.* (2012) Munc18b is an essential gene in mice whose expression is limiting for secretion by airway epithelial and mast cells. *Biochem. J.* **446,** 383–394 CrossRef Medline
22. Gutierrez, B. A., Chavez, M. A., Rodarte, A. I., Ramos, M. A., Dominguez, A., Petrova, Y., Davalos, A. J., Costa, R. M., Elizondo, R., Tuvim, M. J., Dickey, B. F., Burns, A. R., Heidelberger, R., and Adachi, R. (2018) Munc18-2, but not Munc18-1 or Munc18-3, controls compound and single-vesicle-regulated exocytosis in mast cells. *J. Biol. Chem.* **293,** 7148–7159 CrossRef Medline
23. Blank, U., Cyprien, B., Martin-Verdeaux, S., Paumet, F., Pombo, I., Rivera, J., Roa, M., and Varin-Blank, N. (2002) SNAREs and associated regulators in the control of exocytosis in the RBL-2H3 mast cell line. *Mol. Immunol.* **38,** 1341–1345 CrossRef Medline
24. Woska, J. R., Jr., and Gillespie, M. E. (2012) SNARE complex-mediated degranulation in mast cells. *J. Cell. Mol. Med.* **16,** 649–656 CrossRef Medline
25. Paumet, F., Le Mao, J., Martin, S., Galli, T., David, B., Blank, U., and Roa, M. (2000) Soluble NSF attachment protein receptors (SNAREs) in RBL-2H3 mast cells: functional role of syntaxin 4 in exocytosis and identification of a vesicle-associated membrane protein 8-containing secretory compartment. *J. Immunol.* **164,** 5850–5857 CrossRef Medline
26. Puri, N., and Roche, P. A. (2006) Ternary SNARE complexes are enriched in lipid rafts during mast cell exocytosis. *Traffic* **7,** 1482–1494 CrossRef Medline
27. Woska, J. R., Jr., and Gillespie, M. E. (2011) Small-interfering RNA-mediated identification and regulation of the ternary SNARE complex mediating RBL-2H3 mast cell degranulation. *Scand. J. Immunol.* **73,** 8–17 CrossRef Medline
28. Liu, S., Nugroho, A. E., Shudou, M., and Maeyama, K. (2012) Regulation of mucosal mast cell activation by short interfering RNAs targeting syntaxin4. *Immunol. Cell Biol.* **90,** 337–345 CrossRef Medline
29. Naskar, P., Naqvi, N., and Puri, N. (2018) Blocking dephosphorylation at serine 120 residue in t-SNARE SNAP-23 leads to massive inhibition in exocytosis from mast cells. *J. Biosci.* **43,** 127–138 CrossRef Medline
30. Salinas, E., Quintanar-Stephano, A., Córdova, L. E., and Ouintanar, J. L. (2008) Allergen-sensitization increases mast-cell expression of the exocytotic proteins SNAP-23 and syntaxin 4, which are involved in histamine secretion. *J. Investig. Allergol. Clin. Immunol.* **18,** 366–371 Medline
31. Sander, L. E., Frank, S. P., Bolat, S., Blank, U., Galli, T., Bigalke, H., Bischoff, S. C., and Lorentz, A. (2008) Vesicle associated membrane protein (VAMP)-7 and VAMP-8, but not VAMP-2 or VAMP-3, are required for activation-induced degranulation of mature human mast cells. *Eur. J. Immunol.* **38,** 855–863 CrossRef Medline
32. Tadokoro, S., Nakanishi, M., and Hirashima, N. (2010) Complexin II regulates degranulation in RBL-2H3 cells by interacting with SNARE complex containing syntaxin-3. *Cell. Immunol.* **261,** 51–56 CrossRef Medline
33. Tadokoro, S., Nakanishi, M., and Hirashima, N. (2005) Complexin II facilitates exocytotic release in mast cells by enhancing Ca^{2+} sensitivity of the fusion process. *J. Cell Sci.* **118,** 2239–2246 CrossRef Medline
34. Martin-Verdeaux, S., Pombo, I., Iannascoli, B., Roa, M., Varin-Blank, N., Rivera, J., and Blank, U. (2003) Evidence of a role for Munc18–2 and microtubules in mast cell granule exocytosis. *J. Cell Sci.* **116,** 325–334 CrossRef Medline
35. Hibi, T., Hirashima, N., and Nakanishi, M. (2000) Rat basophilic leukemia cells express syntaxin-3 and VAMP-7 in granule membranes. *Biochem. Biophys. Res. Commun.* **271,** 36–41 CrossRef Medline
36. Tadokoro, S., Kurimoto, T., Nakanishi, M., and Hirashima, N. (2007) Munc18-2 regulates exocytotic membrane fusion positively interacting with syntaxin-3 in RBL-2H3 cells. *Mol. Immunol.* **44,** 3427–3433 CrossRef Medline
37. Brochetta, C., Suzuki, R., Vita, F., Soranzo, M. R., Claver, J., Madjene, L. C., Attout, T., Vitte, J., Varin-Blank, N., Zabucchi, G., Rivera, J., and Blank, U. (2014) Munc18-2 and syntaxin 3 control distinct essential steps in mast cell degranulation. *J. Immunol.* **192,** 41–51 CrossRef Medline
38. Bin, N. R., Jung, C. H., Kim, B., Chandrasegram, P., Turlova, E., Zhu, D., Gaisano, H. Y., Sun, H. S., and Sugita, S. (2015) Chaperoning of closed

syntaxin-3 through Lys46 and Glu59 in domain 1 of Munc18 proteins is indispensable for mast cell exocytosis. *J. Cell Sci.* **128,** 1946–1960 CrossRef Medline
39. Tadokoro, S., Shibata, T., Inoh, Y., Amano, T., Nakanishi, M., Hirashima, N., and Utsunomiya-Tate, N. (2016) Phosphorylation of syntaxin-3 at Thr 14 negatively regulates exocytosis in RBL-2H3 mast cells. *Cell Biol. Int.* **40,** 589–596 CrossRef Medline
40. Frank, S. P., Thon, K. P., Bischoff, S. C., and Lorentz, A. (2011) SNAP-23 and syntaxin-3 are required for chemokine release by mature human mast cells. *Mol. Immunol.* **49,** 353–358 CrossRef Medline
41. Baram, D., Adachi, R., Medalia, O., Tuvim, M., Dickey, B. F., Mekori, Y. A., and Sagi-Eisenberg, R. (1999) Synaptotagmin II negatively regulates Ca^{2+}-triggered exocytosis of lysosomes in mast cells. *J. Exp. Med.* **189,** 1649–1658 CrossRef Medline
42. Bin, N. R., Jung, C. H., Piggott, C., and Sugita, S. (2013) Crucial role of the hydrophobic pocket region of Munc18 protein in mast cell degranulation. *Proc. Natl. Acad. Sci. U.S.A.* **110,** 4610–4615 CrossRef Medline
43. Adhikari, P., and Xu, H. (2018) PKC-dependent phosphorylation of Munc18a at Ser313 in activated RBL-2H3 cells. *Inflamm. Res.* **67,** 1–3 CrossRef Medline
44. Vardar, G., Chang, S., Arancillo, M., Wu, Y. J., Trimbuch, T., and Rosenmund, C. (2016) Distinct functions of syntaxin-1 in neuronal maintenance, synaptic vesicle docking, and fusion in mouse neurons. *J. Neurosci.* **36,** 7911–7924 CrossRef Medline
45. Fernandez, J. M., Neher, E., and Gomperts, B. D. (1984) Capacitance measurements reveal stepwise fusion events in degranulating mast cells. *Nature* **312,** 453–455 CrossRef Medline
46. Alvarez de Toledo, G., and Fernandez, J. M. (1990) Patch-clamp measurements reveal multimodal distribution of granule sizes in rat mast cells. *J. Cell Biol.* **110,** 1033–1039 CrossRef Medline
47. Helander, H. F., and Bloom, G. D. (1974) Quantitative analysis of mast cell structure. *J. Microsc.* **100,** 315–321 CrossRef Medline
48. Zimmerberg, J., Curran, M., Cohen, F. S., and Brodwick, M. (1987) Simultaneous electrical and optical measurements show that membrane fusion precedes secretory granule swelling during exocytosis of beige mouse mast cells. *Proc. Natl. Acad. Sci. U.S.A.* **84,** 1585–1589 CrossRef Medline
49. Royet, J. P. (1991) Stereology: a method for analyzing images. *Prog. Neurobiol.* **37,** 433–474 CrossRef Medline
50. Kraeuter Kops, S., Theoharides, T. C., Cronin, C. T., Kashgarian, M. G., and Askenase, P. W. (1990) Ultrastructural characteristics of rat peritoneal mast cells undergoing differential release of serotonin without histamine and without degranulation. *Cell Tissue Res.* **262,** 415–424 CrossRef Medline
51. Azouz, N. P., Zur, N., Efergan, A., Ohbayashi, N., Fukuda, M., Amihai, D., Hammel, I., Rothenberg, M. E., and Sagi-Eisenberg, R. (2014) Rab5 is a novel regulator of mast cell secretory granules: impact on size, cargo, and exocytosis. *J. Immunol.* **192,** 4043–4053 CrossRef Medline
52. Wendler, F., Page, L., Urbé, S., and Tooze, S. A. (2001) Homotypic fusion of immature secretory granules during maturation requires syntaxin 6. *Mol. Biol. Cell* **12,** 1699–1709 CrossRef Medline
53. Makabe-Kobayashi, Y., Hori, Y., Adachi, T., Ishigaki-Suzuki, S., Kikuchi, Y., Kagaya, Y., Shirato, K., Nagy, A., Ujike, A., Takai, T., Watanabe, T., and Ohtsu, H. (2002) The control effect of histamine on body temperature and respiratory function in IgE-dependent systemic anaphylaxis. *J. Allergy Clin. Immunol.* **110,** 298–303 CrossRef Medline
54. Strait, R. T., Morris, S. C., Yang, M., Qu, X. W., and Finkelman, F. D. (2002) Pathways of anaphylaxis in the mouse. *J. Allergy Clin. Immunol.* **109,** 658–668 CrossRef Medline
55. Dombrowicz, D., Flamand, V., Miyajima, I., Ravetch, J. V., Galli, S. J., and Kinet, J. P. (1997) Absence of Fc ϵRI α chain results in upregulation of Fc γRIII-dependent mast cell degranulation and anaphylaxis: evidence of competition between Fc ϵRI and Fc γRIII for limiting amounts of FcR β and γ chains. *J. Clin. Invest.* **99,** 915–925 CrossRef Medline
56. Suzuki, K., and Verma, I. M. (2008) Phosphorylation of SNAP-23 by IκB kinase 2 regulates mast cell degranulation. *Cell* **134,** 485–495 CrossRef Medline
57. Tiwari, N., Wang, C. C., Brochetta, C., Ke, G., Vita, F., Qi, Z., Rivera, J., Soranzo, M. R., Zabucchi, G., Hong, W., and Blank, U. (2008) VAMP-8 segregates mast cell-preformed mediator exocytosis from cytokine trafficking pathways. *Blood* **111,** 3665–3674 CrossRef Medline
58. Yang, Y., Kong, B., Jung, Y., Park, J. B., Oh, J. M., Hwang, J., Cho, J. Y., and Kweon, D. H. (2018) Soluble *N*-ethylmaleimide-sensitive factor attachment protein receptor-derived peptides for regulation of mast cell degranulation. *Front. Immunol.* **9,** 725 CrossRef Medline
59. Tamori, Y., Kawanishi, M., Niki, T., Shinoda, H., Araki, S., Okazawa, H., and Kasuga, M. (1998) Inhibition of insulin-induced GLUT4 translocation by Munc18c through interaction with syntaxin4 in 3T3-L1 adipocytes. *J. Biol. Chem.* **273,** 19740–19746 CrossRef Medline
60. Tellam, J. T., Macaulay, S. L., McIntosh, S., Hewish, D. R., Ward, C. W., and James, D. E. (1997) Characterization of Munc-18c and syntaxin-4 in 3T3-L1 adipocytes: putative role in insulin-dependent movement of GLUT-4. *J. Biol. Chem.* **272,** 6179–6186 CrossRef Medline
61. Morey, C., Kienle, C. N., Klöpper, T. H., Burkhardt, P., and Fasshauer, D. (2017) Evidence for a conserved inhibitory binding mode between the membrane fusion assembly factors Munc18 and syntaxin in animals. *J. Biol. Chem.* **292,** 20449–20460 CrossRef Medline
62. Hackmann, Y., Graham, S. C., Ehl, S., Höning, S., Lehmberg, K., Aricò, M., Owen, D. J., and Griffiths, G. M. (2013) Syntaxin binding mechanism and disease-causing mutations in Munc18-2. *Proc. Natl. Acad. Sci. U.S.A.* **110,** E4482–E4491 CrossRef Medline
63. Blank, U. (2011) The mechanisms of exocytosis in mast cells. *Adv. Exp. Med. Biol.* **716,** 107–122 CrossRef Medline
64. Dernick, G., de Toledo, G. A., and Lindau, M. (2007) The patch amperometry technique: design of a method to study exocytosis of single vesicles. in *Electrochemical Methods for Neuroscience* (Michael, A. C., and Borland, L. M., eds) pp. 315–336, CRC Press/Taylor & Francis, Boca Raton, FL
65. Dieckmann, N. M., Hackmann, Y., Aricò, M., and Griffiths, G. M. (2015) Munc18-2 is required for syntaxin 11 localization on the plasma membrane in cytotoxic T-lymphocytes. *Traffic* **16,** 1330–1341 CrossRef Medline
66. Wu, L. G., Hamid, E., Shin, W., and Chiang, H. C. (2014) Exocytosis and endocytosis: modes, functions, and coupling mechanisms. *Annu. Rev. Physiol.* **76,** 301–331 CrossRef Medline
67. Scholten, J., Hartmann, K., Gerbaulet, A., Krieg, T., Müller, W., Testa, G., and Roers, A. (2008) Mast cell-specific Cre/loxP-mediated recombination *in vivo*. *Transgenic Res.* **17,** 307–315 CrossRef Medline
68. Schnütgen, F., De-Zolt, S., Van Sloun, P., Hollatz, M., Floss, T., Hansen, J., Altschmied, J., Seisenberger, C., Ghyselinck, N. B., Ruiz, P., Chambon, P., Wurst, W., and von Melchner, H. (2005) Genomewide production of multipurpose alleles for the functional analysis of the mouse genome. *Proc. Natl. Acad. Sci. U.S.A.* **102,** 7221–7226 CrossRef Medline
69. Schwenk, F., Baron, U., and Rajewsky, K. (1995) A cre-transgenic mouse strain for the ubiquitous deletion of loxP-flanked gene segments including deletion in germ cells. *Nucleic Acids Res.* **23,** 5080–5081 CrossRef Medline
70. Adachi, R., Krilis, S. A., Nigrovic, P. A., Hamilton, M. J., Chung, K., Thakurdas, S. M., Boyce, J. A., Anderson, P., and Stevens, R. L. (2012) Ras guanine nucleotide-releasing protein-4 (RasGRP4) involvement in experimental arthritis and colitis. *J. Biol. Chem.* **287,** 20047–20055 CrossRef Medline
71. Tschanz, S. A., Burri, P. H., and Weibel, E. R. (2011) A simple tool for stereological assessment of digital images: the STEPanizer. *J. Microsc.* **243,** 47–59 CrossRef Medline
72. Ochs, M. (2006) A brief update on lung stereology. *J. Microsc.* **222,** 188–200 CrossRef Medline
73. Lindau, M., and Neher, E. (1988) Patch-clamp techniques for time-resolved capacitance measurements in single cells. *Pflugers Arch.* **411,** 137–146 CrossRef Medline